Investigating effects of sensor fusion of multiple combinations of sensors on Robotic localisation uncertainty.

Janek Zimoch, Andreas Giobazolias, John Girousis, and Vladimir Mozhaev[1]

***Abstract*— This paper aims to explore performance improvements of using sensor fusion of gyroscope and magnetometer over wheel encoder odometry's (WEO) localisation estimates (x and y position on a 2D map). In order to explore this topic two sources of systematic error are introduced by varying effective wheelbase and wheel diameter dimensions. Pololu Romi 32U4 robot is asked to complete the uni-directional rectangular path test map [4] while four different kinematic models log its perceived localisation. Sensor fusions of 'magnetometer + WEO' as well as 'gyroscope + WEO' are found insufficient to improve localisation performance in this experiment. Sensor fusion of 'magnetometer + gyroscope + WEO' has been found to produce better Mean Absolute Error score than a simple WEO model, when +/- 6% effective wheelbase error or +/- 3% wheelbase diameter error were present. It is concluded that sensor fusion of gyroscope and magnetometer can be beneficial to localisation efforts, however use of sensors with higher measurement precision, as well as use of more advanced, dynamic, adaptive filters to combine heading measurements are necessary for larger and more robust improvements.**

I. INTRODUCTION

Differential drive robot's ability to keep track of its location (spatial coordinate position and heading angle) is an essential part in mapping and SLAM (simultaneous localization and mapping) problems. Localisation errors accumulate as the robot moves. Environmental features are mapped based on the robot position, so an improvement in localisation and decreased systematic errors directly affect mapping quality. A robotic system which does a poor job at updating its location will accumulate error over time, introducing bias to every future mapping activity. Fortunately, self-localisation by robotic systems can be improved. One common approach is via sensor fusion, where measurements from sensors like gyroscope and magnetometer can be combined with wheel encoder-based odometry (WEO) to reduce uncertainty in robot's localisation perception.

In this paper, we investigate improvements gyroscope and magnetometer can bring to robot's localisation when integrated with wheel encoder odometry (WEO) via complimentary sensor fusion. Alpha-beta filters (or GH-filters) will be used to fuse sensors with WEO and three different variations of sensor combinations will be tested: Magnetometer + WEO, Gyroscope + WEO, Magnetometer + Gyroscope + WEO via Alpha-Beta-Gamma (GH filter and complimentary filter). Through study of different variations of sensor fusion we hope to improve our understanding of relative advantages and disadvantages of each method. It is expected for the gyroscope to perform better in short term and magnetometer in long term (due to gyroscope's drift). We also hypothesize that the effective improvement in localisation of combined Magnetometer with Gyroscope will be smaller than the sum of the gains they produced when implemented separately. This may be true because each sensor helps to reduce a certain type of error in localisation. Therefore, when two or more sensors are used alongside each other, the scope where each of them is helpful may overlap [1].

To test the improvements in localisation performance using various instances of sensor fusion, different sources of error are introduced. The focus of this work will be on systematic sources of error, especially: effective wheelbase and wheel diameter. Magnitude of this errors will be controlled in hopes to reveal more information about the performance gain of sensor fusion. The experiment aims to produce data that can be generalised, which can be used and applied directly for any further sensor fusion work.

II. SOURCES OF ERROR - WHEEL ENCODER ODOMETRY

Gyroscope and magnetometer can help reduce certain types of errors in localisation that arise when wheel encoder odometry is used. Presence and magnitude of each of those errors is dependent on the course the robot is asked to follow as well as the accuracy with which robotic system was manufactured and characterised (i.e. wheel diameters, wheel alignment). Therefore, depending on the robot and the task that the robot is asked to perform, the gain from sensor fusion will vary.

It is inferred that to produce reproducible results which would be useful to research community, sensor fusion gains need to be investigated with respect to a specific source of error that is limiting WEO.

Error sources in wheel encoder odometry can be divided into systematic and non-systematic [3] [4]:

1) Systematic error sources:

- Unequal wheel diameters
- Effective wheelbase dimension
- Average of both wheel diameters differs from nominal diameter
- Misalignment of wheels
- Limited encoder resolution and sampling rate

[1] (All) Department of Mechanical Engineering, University of Bristol

*GitHub repository with code and maps is available under this link: github.com/janekzimoch/Robotics_Systems_2019

2) Non-systematic error sources:

- Wheel-slippage (due to slippery floors, over-acceleration, fast turning (skidding), external forces such as interaction with external bodies) or non-point wheel contact with floor
- Travel on uneven terrain or over obstacles

A robotic system can also experience localisation errors due to approximations in mathematical models used for odometry. However, these errors tend to be be negligible for robotic systems traveling at speeds $< 1m/s$ and with encoder sampling lower than every 10ms [4].

A. Error sources considered in this work

Because of the time constraint on conducting this research as well as relevance of error sources to studied robotic system, the following error sources will be considered in this study:

- Systematic:
  - Effective wheelbase dimension
  - Unequal wheel dimension

It was decided to focus solely on systematic sources of error, because for flat environments these tend to be the most significant as they keep accumulating constantly, they can be more accurately described and such experiments are more repeatable [4]. "Misalignment of wheels" source of error was omitted, as it is hard to control it in the robot used in this study. "Limited encoder sampling rate" and "Limited encoder resolution" were first investigated in a preliminary experiment but then dropped, for explanation see Section VII. "Map - A. Preliminary Map".

III. ROBOTIC SYSTEM

In this work, a Pololu Romi 32U4 Control Board was used, which uses the Arduino-compatible ATmega32U4 micro-controller unit (Fig. 1).

The robot is equipped with:

- Two Encoders, monitoring the encoder counts of the wheels
- LIS3MDL 3-axis Magnetometer, positioned at the front part of the Romi on a mount.
- 3-point IR (line) sensor, positioned the front of the Romi underneath the wheel axle.
- Gyroscope, single Inertial Measurement Unit (LSM6DS33 IMU) integrated into the control board

IV. DISTORTED MAGNETIC FIELD

In a study [12] which also looked into sensor fusion, authors point out that due to close proximity of DC motors to their magnetometer, the sensor could not provide accurate measurements, as the magnetic field created by motors and other electronics distorted the magnetic field of the earth. Therefore, a preliminary experiment was performed to observe and mitigate errors from the magnetic field created by our system. Specifically, the primary source of magnetic field was the two DC motors and thus different positions

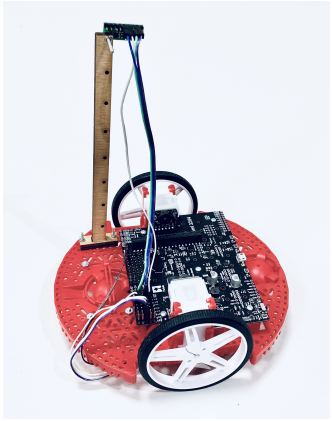

Fig. 1: Pololu Romi 32U4 robot used in this work (with magnetometer mount)

of the magnetometer were tested. The results demonstrated a minimum distortion of the magnetometer's reading within the bisector of the two wheel and as far away from the axis of their rotation.

To reduce the effect of this systematic yet non-constant error, it was decided to elevate the magnetometer on a mount. The theory that this would improve the readings was confirmed and as the magnetometer was mounted higher, the steady-state error due to motors running (while the Romi was stationary) decreased in every axis, as can be seen in Figure 2. Therefore, it was chosen to mount the magnetometer at the highest setting (160 mm) (as seen in Figure 1.

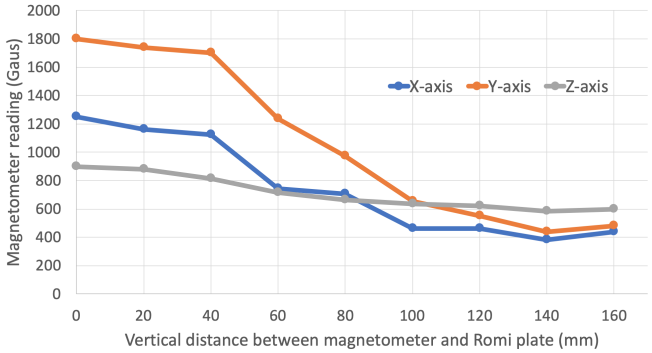

Fig. 2: Magnetometer reading variation with elevation

V. CONTROL OF SYSTEMATIC ERRORS

A. Effective wheelbase

In many robotic systems effective wheelbase is affected by the fact that rubber tires contact the floor not in one point, but rather in a contact area [4]. Wheel separation of the robot used in this work is 140 mm, and is not expected to vary as wheels are narrow and will not undergo compression as the loads present are low. Therefore, the error was introduced in the software instead of hardware. A "wheel separation" parameter in the mathematical model of kinematics responsible for calculating localisation will be adjusted from 140mm by different bias terms: +4mm, +8mm,

0, -4mm and -8mm. As the result, robot's perception of it's wheelbase will be different to the actual separation. Thus, mathematical model will keep accumulating localisation error as the robot goes through the course.

B. Unequal wheel dimension

In general, two similar rubber tires can have different diameter due to complexity of their manufacturing and due to compression by asymmetric load distribution. In presented robotic system, wheel diameters were measured using vernier caliper with accuracy of 0.1 mm, and they were both find to be 70.0 mm. Furthermore, loads present in the study are not expected to alter wheel dimensions as they will be too low too compress tires. Therefore, to vary wheel diameter for the purpose of the experiment a tape was wrapped around left and right wheel to control their diameter. It has been decided to test following variations in wheel diameter: +2mm Left wheel, +1mm Left wheel, +0mm, +1mm Right wheel, +2mm Right wheel (when modifying one diameter the other was kept constant). By modifying diameter it is expected that the robot will produce biased perception of its localisation. The total encoder counts of the wheel with larger diameter is going to be smaller than of the other wheel. Therefore, despite robot going straight, the WEO model should predict that the robot was turning slightly towards the side of larger wheel.

VI. KINEMATIC MODELS

To test the effectiveness of gyroscope and magnetometer at reducing localisation error via sensor fusion, four variations of Kinematic model were tested:

1) Baseline: WEO
2) GH filter: WEO + Gyroscope (or GWEO)
3) GH filter: WEO + Magnetometer (MWEO)
4) GH filter: WEO + Complimentary reading of [Gyroscope + Magnetometer] (COWEO)

The variation to kinematic model is made by changing the way it calculates robot's pose (heading angle - theta). The baseline model uses solely WEO to estimate heading, while the remaining three implementations use a GH filter to complement measurements of WEO with measurements of external sensors: gyroscope and magnetometer. The following 4 sections explain how each Kinematic model was implemented.

A. Baseline: WEO

Using only wheel encoder odometry, a simple kinematics system is implemented that is used as the baseline experiment. By knowing the size of the wheels and wheelbase, it is possible to calculate the distance travelled in forward direction (δx) and the angle (θ) relating to the heading at the start of Romi's run. c_1 and c_2 are the encoder counts from each wheel converted to radians, while d is separation between the wheels. New values for: angle, x, and y are then calculated.

$$\delta x = \frac{(c_1 * r_{wheel}) + (c_2 * r_{wheel})}{2} \tag{1}$$

$$\delta\theta = \frac{(c_1 * r_{wheel}) - (c_2 * r_{wheel})}{d} \tag{2}$$

$$x_t = x_{t-1} + (\delta X * cos(\theta + \delta\theta)) \tag{3}$$

$$y_t = y_{t-1} + (\delta X * sin(\theta + \delta\theta)) \tag{4}$$

B. GH filter

Here a general implementation of GH filter is presented which is shared across all 3 sensor fusion implementations (GWEO, MWEO, COWEO).

First an estimate of angular velocity, $\omega_{estimate}$, is computed using both the previous estimate and the new angular velocity calculated using WEO. An extra parameter β is used, the magnitude of which relates to the precision of ω_{WEO}. If values of ω_{WEO} are precise and trusted, β should be close to 1, otherwise close to 0.

$$\omega_{estimate} = \omega_{estimate,t-1} \ + \ \beta * \omega_{WEO} \tag{5}$$

The estimated angular velocity is now integrated and corrected using sensor measurements, as presented in equation 6. The result of the equation is θ_{pred} and it represents the predicted heading angle.

$$\theta_{pred} = \theta_{pred,\ t-1} \ + \ \alpha * (\omega_{estimate} * \delta t - \theta_{sensors}) \tag{6}$$

C. GH filter: WEO + Gyroscope

1) Calibration: The first stage of using the gyroscope is to correctly calibrate it to get rid of any inherit errors. This is done by taking 50 readings at each axis at 50 ms intervals and then averaging them to calculate the offset from zero. It is necessary for the Romi to be still to prevent introducing any wrong measurements. This offset is then subtracted from all subsequent readings of the gyroscope.

2) Sensor fusion: Gyroscope's signal can be interpreted as robot's angular velocity. Therefore, to find angular change of heading, the signal is integrated with respect to time. It is then used to correct WEO heading angle estimate via GH filter, see equation (6) in previous section, where $\theta_{sensors}$ represents calibrated readings of gyroscope and parameter α specifies our confidence level in gyroscopes readings. Values close to 1 indicate that gyroscope produces more valuable estimates than WEO, while values closer to 0 indicate otherwise.

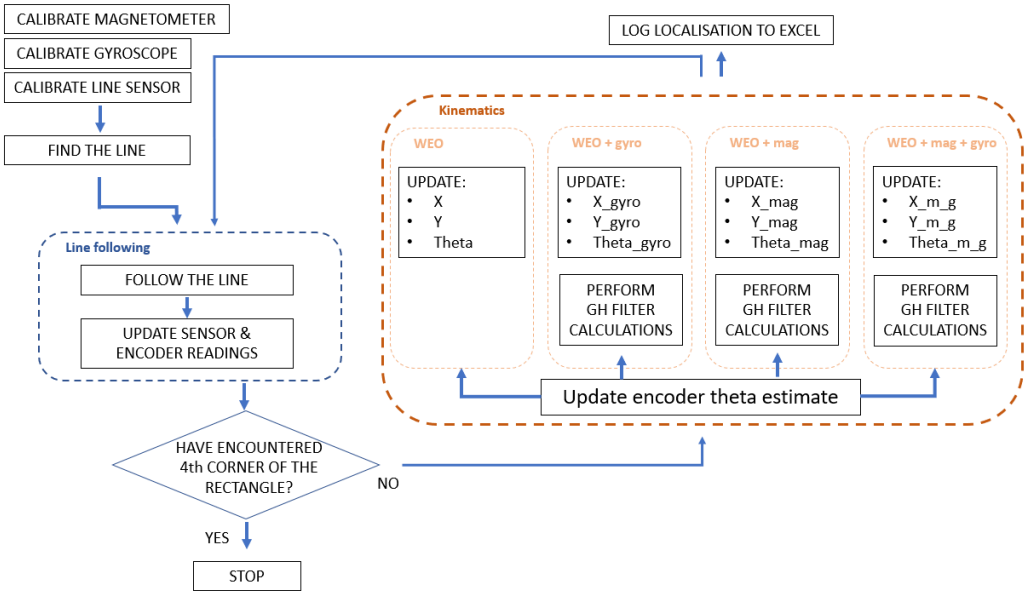

Fig. 3: System architecture showing two main parts of the system: Kinematics - responsible for creating data on robot's perception of localisation, and Line following - responsible for making the robot complete the rectangular test map. The code terminates, after robot successfully completed a full rectangular map. Schematic displays a single loop which runs until termination. Every loop iteration (or about every 10 ms) localisation data of each kinematic model is logged to excel.

D. GH filter: WEO + Magnetometer

1) Calibration: Magnetometer is calibrated similarly, however as it is more sensitive to noise (such as magnetic objects around), the offset is calculated as the average between minimum and maximum readings, and the range of readings for each axis is obtained. This allows to scale the readings from each axis so they have the same sensitivity. During magnetometer calibration, Romi has to be rotated through 360 degrees in each axis in order to detect any peaks or troughs in readings.

2) Sensor fusion: Magnetometer measures strength of magnetic field in x, y, and z direction. To extract useful information about robot's yaw angle following equation had to be used:

$$\theta_{magnetometer} = arctan(\frac{B_x}{B_y}) \tag{7}$$

Where B_x is the Magnetic field flux in x-direction (ahead of the robot), and B_z is the Magnetic field flux in y-direction (laterally to the position of the robot). Magnetometer heading measurement had high levels of high frequency noise therefore a low pass filter was implemented to smooth them out.

E. GH filter: WEO + Magnetometer + Gyro

1) Complementary equation: Heading measurements of gyroscope and magnetometer can be combined via complementary filter. This is expected to provide an improved measurement of the heading angle. Gyroscope is considered accurate in short term, however it cannot be trusted in long term as it's reading are susceptible to drift (accuracy diminishes over time) [10]. Magnetometer doesn't have the drift problem but is considered less accurate than gyroscope in short term. Complementary equation which combines readings of both sensors is presented below.

$$\theta_{comp} = (1-\gamma)\theta_{mag} + \gamma\theta_{gyro} \tag{8}$$

γ is a constant, ranging from 0 to 1, which determines the relative weight given to each of the two sensors. If gyroscope readings are more trusted than readings of a magnetometer, then γ should be greater than 0.5.

2) Sensor fusion: For this Kinematic model, the GH filter is used in a similar fashion. However this time $\theta_{sensors}$ represents the combination of magnetometer and gyroscope readings θ_{comp}.

VII. MAP

It is desired to measure localisation performance of Kinematic models presented in previous section with respect to a specific source of error:

- Effective wheelbase dimension
- Unequal wheel dimension
- Encoder resolution and sampling rate (dropped in final experiments)

In order to ensure that the examined errors are isolated and no other sources of error affect the experiment (i.e. wheel-slippage), the course was decided to be as simple as possible. A straight line was considered, yet this would not allow for some tested sources of error to affect localisation (i.e. errors in effective wheelbase separation don't affect localisation on straight line). Therefore the map has to include some curvature or turns. Additionally, the objective of this study is

to produce reproducible and easy-to-generalise results which can be useful for the research community - this motivated use of a standard map, used in similar studies by other researchers in the past. We decided to use a rectangular map with 90 deg corners, similar to the "uni-directional square path test map" used other researchers [4]. The dimensions of the map are 600 mm in X-direction and 1000 mm in Y-direction, seen in Figure 4.

A. Preliminary map - curve with constant curvature

Initially, it was decided to verify the experimental procedure using a simple map, before moving onto the uni-directional square path test map.This simplified problem was expected to reveal any imperfections in the experimental procedure and the code, as well as provide better understanding of localisation and sensor fusion topics. For the simplified preliminary experiment a curve of constant 0.5m radius of curvature and can be seen in Figure 4.

Following the preliminary experiment following observations were drawn:

"Encoder resolution" systematic error was tested. Following encoder resolutions were tested: 1440, 720, 360 (these were obtained through software adjustments). Yet, these were found to be a very minor source of error and it was decided to be omitted entirely. Similarly, error source "Encoder sampling rate" was also omitted.

Improvement of localisation due to sensor fusion was far from decisive, as it often performed worse than WEO by itself. Yet, based on background literature review this was expected.

However, the single constant curvature map failed to produce significant errors, which further reinforced belief in using a map similar to the "uni-directional square test map".

It was hard to distinguish between sources of errors based on produced results (the two types, A and B [[4]] are discussed in Section XII). Therefore, the need for a map similar to the "uni-directional square test map" was further reinforced as it is expected for the one type of error (A) to accumulate at the 90 degree turns, and a different type (B) to accumulate over straight lines, making them easier to distinguish and analyse.

B. Proper map - uni-directional rectangular path

It has been decided to use a rectangular map as presented in Figure 4.

This map includes four 90 degree corners which will make it easy to evaluate errors accumulated during turning. Additionally, the map starts and finishes at the same point, thus it will allow to easily track robot's final localisation error - i.e. how much does the position deviate from the origin after map is completed. Finally, it is similar to the "uni-directional square path test" often used in localisation and sensor fusion research, making it easy to replicate the experiment.

VIII. EXPERIMENTAL PROCEDURE

This section explains the experimental procedure and to show how data was collected, building on the information

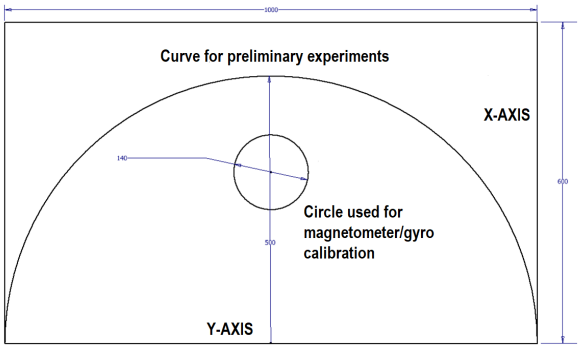

Fig. 4: A course used to conduct experiments

mentioned already in previous sections: "Control of Systematic Errors", "Kinematic Models", "Map".

A. Path traversal

The robot was asked to follow a line using a line sensor, effectively completing a path of rectangular shape. During its traversal through the path, robot would log it's perception of its localisation in real time. Then these logged results can be compared against the actual path, fixed by the black line it was following. This approach was chosen over a hard-coded path within the robot because it would eliminate the need to take error measurements in the physical world as the path would only be affected in the software.

B. Experimental trials

Table 1 presents 4 different "Experiment types", where each type differs from others by the source of error that was introduced. Column two presents what variable was controlled to vary the magnitude of the introduced error. It has been decided to conduct 10 experimental trial for each control parameter which gives total of: $10*(1+4+4+3) = 120$ trials. During each trial the robot will complete a full rectangular path by following the black line.

TABLE I: Column 1 lists baseline experiments conducted for this work. Column 2 lists control parameter for each experiment

Experiment types:	Control parameter
1. No Error :	N/A
2. Wheelbase:	Effective Wheelbase: -8mm, -4mm, +4mm, +8mm
3. Wheel diameter:	Right Wheel: +2mm, +1mm; Left wheel: +1mm, +2mm

C. Localisation data acquisition

During the trial all four Kinematic Models (presented in the Section V. Kinematic Models) will be active, each creating its own, independent perception of robot's localisation. This is possible because localisation data is not used by the

robot in any way while traversing the course - as the robot uses solely line sensor to follow the rectangular path.

During every trial each Kinematic model logged its perceived localisation data (x, y coordinates) every 10 ms to a spreadsheet. PLX-DAQ software was used to import data via cable to Microsoft Excel on a computer in real time. Each trial produced approximately 2000 x and y data rows. After 10 trials were conducted for each experimental scenario, 10 data points from across the trials that related to the same location on the map were averaged to produce a mean path (elaborated in Section XI). This approach is expected remove any random error that could be present in individual trials, making the results more robust and reliable.

IX. PERFORMANCE METRICS

It has been decided to approach result analysis from both quantitative and qualitative perspective.

A. Quantitative - MAE

It is desired to use a single value performance metric to evaluate performance of each kinematic model during every experimental scenario. Such single value, if effective at quantifying kinematic model's localisation performance, would be useful to compare different models against each other, and therefore providing easily comprehensible information of relative performance of different sensor fusion instances.

Assuming that the definition of effective localisation is for the robot's perception of its x-y localisation to agree with its true location, then it is reasonable to use absolute distance metric for calculating the error. The closer robot believes it is to its actual position, the better its performance.

Additionally, such single value metric should summarise performance of localisation throughout the map. Assessing performance only at the end of the map or at some specific points would not portray the true performance of the robot. This is because some errors might cancel out as the robot traverses the path. Ideally, some form of error integral should be considered where errors across the entire path are measured.

Based on above analysis it has been decided to use Mean Absolute Error (MAE) as the main quantitative performance metric. Equation for MAE is presented below:

$$MAE = \frac{1}{n}\sum_{i=1}^{n}\sqrt{(x_{i,t}-x_{i,r})^2-(y_{i,t}-y_{i,r})^2} \quad (9)$$

This metric sums up the euclidean distance between every point logged by robot's perception of its localisation (imported using PLX-DAQ software) and the respective actual location of the robot. Afterwards, the sum is divided by n number of points logged to produce an average distance error.

Because points logged by the robot were time dependent (a single data point was logged every 10ms) it was impossible to find exact values of respective actual locations of the robot on the map. Nevertheless, a close approximation could be inferred. Assuming robot was traveling at constant speed the path defined by a black line that robot followed was divided into n points, now every i^{th} point on the path corresponds to every i^{th} point logged through PLX-DAQ.

Finally, it was decided to use MEA with euclidean distance as opposed to any other distance metric as it is the most interpret-able and universal. MAE is preferred to other methods of calculation such as Mean Square Error because the error grows linearly with the distance between two points. Measuring absolute distance errors also prevented distance signs from cancelling out.

B. Qualitative - Perceived-Path deviation form the truth

While quantitative MAE metric is useful to compare relative performance of each of the Kinematic models using numbers, qualitative analysis of data is also needed, especially following the results of preliminary on a curved path where it was found that sensor fusion is not as efficient as expected on reducing localisation uncertainty.

Because of the way data was logged by PLX-DAQ it is possible to create a visualisation of the path of robot's perceived localisation that was logged. Such path visualisations will then be overlayed to easily compare paths produced by different kinematic models. Such qualitative/visual metric for performance assessment will serve two main purposes:

1) show in more detail why the quantitative MAE metric produced the observed results (visual data is easier to interpret for specific points where errors may be larger) and observe trends;
2) answer questions which couldn't be answered quantitatively. Following preliminary experiment, this could be:
   - Which type of error was most prevalent (Such as type A or B)
   - Which part of the map resulted in greatest accumulation of error
   - Were there any unexpected one-off errors

X. TUNING CONSTANTS IN GH FILTER

This is the last section related to experimental setup, discussing the methodology for choosing constant variables for GH filters. In GH filter the g and h constants (often also called α and β) are very important for its overall performance, if poorly chosen they could make GH filter ineffective or even inferior to an original un-adjusted model.

The disadvantage of the GH filter is that it is not dynamic. The constants that define its performance have to be set once and remain fixed thereafter. The interpretation of the constants is as following: "how precise is the encoder heading localisation as compared to precision of sensor measurements". This suggests that GH filter would work well if the precision of encoder localisation could be quantifiable, however it is not. The precision of encoder heading estimation is dependent on magnitude of systematic errors present. Therefore while tuning GH constants for one scenario, the filter might turn out less effective in another where systematic error has different magnitude.

Despite this caveat, due to lack of available time for the project it was decided to tune the filter non-dynamically

regardless. Constant values were tuned for situation where no errors were present - it was decided to choose this case, as the reason for using sensor fusion to complement encoder odometry is only useful when the systematic errors cannot be measured. Thus tuning system for the case when no errors are implemented is more representative of real life scenario.

Tuning procedure was as follows. Romi was asked to follow the experimental map and during this process localisation coordinates were printed. Coordinates were printed for all kinematic models with varying α for each filter (β was kept constant). Tested constant parameter values were: 0.1, 0.3, 0.5, 0.7, 0.9. For each kinematic model the best parameter was chosen based on the lowest MAE metric. Now the α parameter was kept constant at the recently picked value, and the procedure was repeated for varying β. Now when roughly optimal values for both α and β were selected, the entire procedure was repeated. However this time range of tested parameter was reduced as follows: $\alpha-0.1$, $\alpha-0.05$, α, $\alpha+0.05$, $\alpha+0.1$. Here again the best new alpha was selected based on MAE metric. Same process was repeated for β parameter.

This tuning method is not perfect - it finds a local optimum, as α and β are not likely to be independent of each other. However, considering time constraints for this work, this tuning method was accepted under assumption that local optimum lies close to the global optimum.

XI. RESULTS

Following data are evaluated qualitatively based on scatter graphs mapping the robot's perceived location compared to actual square map translated to Cartesian coordinates and quantitatively using Mean Absolute Error as described in section IX. "Performance Metric". To facilitate text, graph and table comprehension, the kinematic model names were used interchangeably:

- WEO (Wheel Encoder Odometry) and Encoder
- GWEO (Gyroscope + WEO fusion) and Gyro
- MWEO (Magnetometer + WEO fusion) - Magnetometer
- COWEO (Magnetometer + Gyro + WEO fusion) - GH

A. NOMINAL - NO INTRODUCED ERROR

TABLE II: Mean Absolute Errors for the trial with no introduced error

Case :	Encoder (mm)	Gyro (mm)	Magnetometer (mm)	GH (mm)
No Error	34.53	111.06	173.92	99.96

The results in table II are treated as a baseline for the experiments. For all cases, the robot is considered to start at (0,0) and the dimensions of the rectangle are 600 by 1000 mm. Any systematic errors that may still be present after calibration and are inherent to the system will be discussed but the aim of the following experiments will be to reject the introduced errors. Inherent systematic errors may still be present but are difficult to quantify with accuracy. Baseline experiments were conducted 10 times and averaged to establish reliable results free from random error.

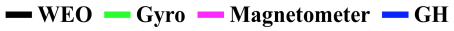

Fig. 5: Legend used for all path visualisations

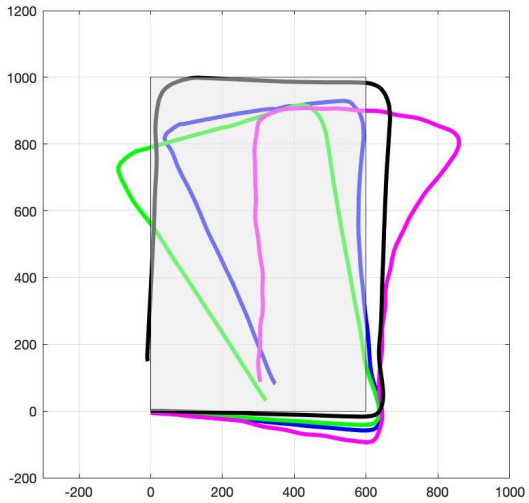

Fig. 6: Robot's perceived localisation paths after following the reference rectangle in the experimental scenario with no systematic error introduced. (distances in mm)

For the nominal case where no systematic error has been introduced encoder odometry has the best performance with a $34.53mm$ MAE, which is 65.4 % lower than the next best performance, GH-filter. These results are expected as sensor fusion of inertial and magnetic methods is reported to be outperformed by encoder odometry for small errors and disturbances [4]. Analysis is also conducted qualitatively based on the scatter map created by the robot. In Figure 6 these maps for the no error scenario are depicted. The encoder results appear to be closer to the desired rectangle as expected from the MAE. The fusion of all sensors in the GH filter allows for the compensation of angle errors in the gyroscope and straight line curvature in the magnetometer, resulting in the next best case after pure encoder odometry.

B. EFFECTIVE WHEELBASE

TABLE III: Effective Wheelbase (WB) Uncertainty Mean Absolute Error data

Case :	Encoders (mm)	Gyro (mm)	Magnetometer (mm)	GH (mm)
WB +4	48.98	162.4	103.6	101.98
WB -4	52.7	138.99	85.61	100.26
WB +8	81.81	89.4	183.68	76.35
WB -8	89.92	118.30	150.6	97.29

Mean Absolute Errors for varying effective wheelbase are presented in Table III. Encoder MAE increases as the

magnitude of wheelbase diameter error is increased (MAE values are of similar magnitude for negative and positive WB error). GWEO and MWEO do not produce consistently low MAE however the combination of the two in the COWEO model has a clear effect with values at least 7.8 % better than individual sensor fusion. GWEO behavior appears similar irrespective of introduced error magnitude. MWEO produces larger error for linear displacements but appears to produce consistent and accurate results for angles of rotation.

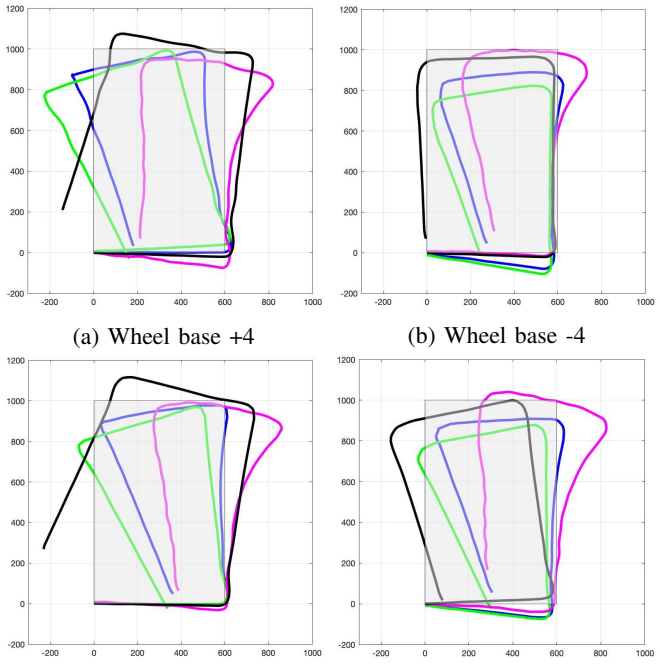

(a) Wheel base +4 (b) Wheel base -4

(c) Wheel base +8 (d) Wheel base -8

Fig. 7: Maps of experiments with adjusted wheel base (distances in mm)

C. EFFECTIVE WHEEL DIAMETER

TABLE IV: Effective Wheel Diameter Mean Absolute Error data

Case :	Encoders (mm)	Gyro (mm)	Magnetometer (mm)	GH (mm)
Ed R+ 1	55.34	78.63	269.47	94.96
Ed L+1	115.48	78.58	169.14	91.08
Ed R+ 2	81.30	80.21	180.9	53.04
Ed L+2	168.74	100.11	179.229	91.29

For errors introduced in the robot wheel diameters, WEO error increases with increase in systematic error magnitude for both left and right wheel. Both GWEO and COWEO produce lower MAE than WEO on its own. MWEO case remains the one with the larger MAE as in previous scenario III,IV,II. Similar to previous cases, examined MWEO angle estimation is consistent but there are curvature errors in the straight line parts of the rectangle. GWEO produce similar geometries as the previous cases but the MAE as mentioned for the wheelbase errors are lower than WEO. It therefore appears that gyroscope angle errors observed in other cases have less of an effect and have not increase with the introduction of wheel diameter uncertainty error.

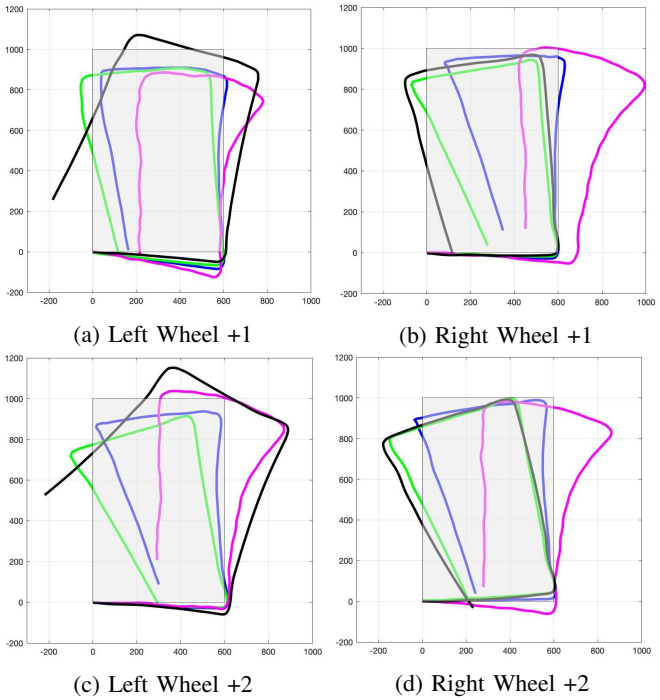

(a) Left Wheel +1 (b) Right Wheel +1

(c) Left Wheel +2 (d) Right Wheel +2

Fig. 8: Maps of experiments with adjusted wheel diameter (distances in mm)

XII. DISCUSSION

A. General discussion

The experiments run produced both quantitative and qualitative data. As expected, COWEO produced less error than MWEO in roughly 90% of cases, and less error than GWEO in approximately 80 % of cases. This is consistent with the initial hypothesis that the combination of gyroscope and magnetometer will perform better than each of these sensors separately. However, MWEO never outperformed pure WEO (from observing both qualitative and quantitative data). This can be explained by relative volatility of the magnetometer readings. Similarly, GWEO in most cases proved less reliable than WEO, although in two cases where the left wheel was made larger, WEO accumulated more error. In order to determine whether the findings are conclusive anticlockwise experiments should be carried out and the pattern examined. If the results are reproducible and reflected in both directions the findings are not direction sensitive. Findings indicate limited benefit from fusing magnetometer and gyroscope with WEO, as expected by the literature. Yet some benefit is evident when a filter is added.

During the ”wheel diameter error” experiments, MAE of COWEO outperformed the one obtained using only WEO, in three out of four cases. During the ”effective wheelbase

error" experiments, however, COWEO produced less error than WEO in four out of five cases. As the error introduced to the wheel diameter and wheel base was increased, the reliability of COWEO in comparison with WEO data increased. Observing the qualitative data, it can be seen that COWEO often produces the most geometrically similar shape to that of the ideal path, especially as the introduced error increased.

To conclude the result analysis, WEO fusion with either magnetometer or gyroscope on their own is not sufficient to improve the localisation of a robotic system.Yet, when COWEO is used the localisation error may be lower than when using WEO on its own. While the collected data makes it difficult to draw conclusive answers about the efficiency of COWEO, there is clearly merit to further research and experimentation as the result provide some hope that with correct optimisation, the localisation of a robotic system can be positively improved.

B. Magnetometer and gyroscope

The difference in source and type of errors for gyroscope and magnetometer fusion provides interesting stepping stones for controller design. COWEO's good response to large systematic errors is hypothesized to be a result of this phenomenon. GWEO produces data that is more robust to small fluctuations in robot's direction and is well suited for straight lines or linear displacements. However, during rotations, especially if they have inconsistent angular velocity, the angles produced by gyroscope seem less predictable. Slow time varying sensor bias observed in gyroscopes due to integration of inherit inconsistencies may be responsible[9].

MWEO data is very sensitive to minor fluctuations and has high-frequency noise present. It is also susceptible to error due to electromagnetic interference such as power supplies or steel structures. Calibration very important, and it is difficult to make the readings reproducible if the environment or orientation of the map is changed. The magnetometer appears to describe the rotations of the robot more accurately, with the angles approximating 90 degrees.

Gyroscope calculates the angle based on previous measurement and the integral of angular velocity, introducing drift. Magnetometer is calculating an angle as it relates to the magnetic fields increasing robustness in long term with respect to absolute heading angle. A conclusion can be drawn that the magnetometer performs more reliably in the long term while the gyroscope is more reliable in short term.

C. Type A and Type B errors

It is assumed that the two types of errors experimented on in this project affect different parts of the localisation and mapping done by WEO. These errors can be broadly categorised as Type A and Type B (terminology introduced J. Borenstein [4]). Changing the wheel base would not result in significant error in WEO-based localisation during straight line travel since each wheel travels the same distance while the heading angle is not affected. However during turns, there would be errors accumulated since the size of the arc of the circle travelled will be affected by diameter of the wheelbase, hence leading to distorted angles. This is categorized as Type A. Type B error would be created due to adjusted wheel diameters. The turning would be affected, but not greatly as the arc of the circle travelled while turning is not significantly larger than the wheel circumference. However, on straight line, the difference in wheel diameter would lead to larger distance being travelled by one wheel, which would skew the robot's perception of its path from a straight line to a curve. The benefit of the square map was that these two errors can be distinguished between.

D. Gyroscope errors

As mentioned before, GWEO performs well on a straight line, but as can be seen across all mapped results, it appears to consistently overestimate the angle of rotations of the path. Thus a large accumulation of error is observed, since a small angle offset will result in progressively larger coordinate errors down the line. The heading estimation is increasingly further from the real angle with each turn, and it becomes obvious at the last straight line of the course (this is often referred to as drift)[5]. Across all of the experiments, this leads to the path created from GWEO being offset to the left (as seen in figures) of the actual path travelled by the robot. This could potentially be explained by several factors.

- Although it has been successfully tested, it is possible that the conversion of angular velocity as measured by gyroscope into angle, in radians, is not perfect. This could be difficult to detect over short term but is a significant systematic error, that could be fixed by extended tuning and testing. Automated stationary gyroscope calibration based on Gaussian-newton smoothing has been proven to work well and could be implemented [9].

- The speed at which the robot turns is not consistent and sometimes appeared 'jerky' as the robot would re-find the line and then lose it again. This could on the short scale (in the range of milliseconds) cause the Romi to constantly change turning speed, which over many dozens of loops could lead to distortions in the angle calculations.

E. Magnetometer errors

Conversely, MWEO angles of turn approximate right angles, but on the straight line there are distortions in one specific part of the path (the vertical line on the right on the map) that can't be attributed to random fluctuations and appear systematic (seen on graphs). Such distortion leads to the accumulation of error, similar to that of GWEO. Interestingly, this error results in the mapped path being offset to the right of the actual course. This can be explained by several potential sources of error.

- It is possible that the map was positioned next to an object that is a source of hard or soft iron error. Due to the location of the map (indoors, in an Engineering building), there could be power supplies, metal fixings, pipes, wires or some metal object placed under the flooring, which would offset the readings of the robot as it travelled next to it. Its vicinity to one side could explain why only one of the path side got skewed.

- Calibrating the magnetometer is difficult to do precisely. On top of that, in the experiments, it was only calibrated for the scenario where the entire pathway of the robot will lie in the same plane as the orientation of the magnetic fields. While typically this approximation is valid for short term and small area experiments, it is possible that there this potential error can decrease the reliability of the results. In order to overcome this problem, it would be necessary to use the accelerometer to calculate the tilt of the robot in relation to the ground, to track its position in 3D environment (in terms of pitch and roll angles). Trigonometric equations can then be used to map the 3D vectors obtained from magnetometer readings onto the 2D plane of the Romi, accounting for its relative alignment with the ground and with the magnetic fields.

F. Further work

As previously described, GWEO and MWEO data are offset due to what appears as systematic errors, but in opposite directions. COWEO, through combining the readings cancels out distortions of both magnetometer and gyro, however it is not clear whether this is a reproducible behaviour or a feature of this particular experimental setup. To explore further it would be beneficial to create different maps in different environments and perform the experiment bidirectionally to eliminate any unforeseen factors that were not controlled.

GH filter is a basic filter where G determines the precision of the measurements we try to correct (WEO) and H determines the precision of the measurements of the sensor data used for making the correction (the closer to 1 the more higher precision/confidence). Arguably the imperfections of sensor fusion are primarily due to sensors limitations rather than due to usefulness of GH filter, however there are other, better approximation algorithms than GH filter. One example is Kalman filter [11], which also considers the estimate uncertainty (Covariance Extrapolation Equation and Covariance Update Equation), therefore allowing for the gains (Kalman Gain) to change over time depending on model and measurement uncertainties. Such dynamic behavior of the filter would allow to better cater for changing conditions and precision of sensors (I.e. drifting gyroscope).

In the preliminary experiment for this work, another filter was tested, GHK filter, where K is a constant term which allows for the system to account for the acceleration when making localisation predictions (GH filter assumes velocity to be constant and acceleration to be 0). However, during the preliminary study the GHK filter has proven inferior to GH filter. This is because it assumes constant acceleration, which could not account for corners of the map where robot's acceleration changed, making the overall localisation approximation unstable.

It is believed that use of more advanced, dynamic filters could improve results of sensor fusion despite limitations of gyroscope and magnetometer. Other filters worth investigating in the future, besides Kalman filter, is Fuzzy filter as well as any other adaptive filter [11]. This would allow for an algorithm to decide which sensors are the most reliable at each instant, and change the weightings assigned to each.

XIII. CONCLUSION

One of the largest problems in robotics is the correspondence (or association) problem, where in order to map the environment, a system needs to localise itself correctly. Since the two are interdependent, it creates complications. This research has mostly concentrated on the "Localisation" part of SLAM problems.

This research showed that both gyroscope and magnetometer, despite their limitations, can be combined together to improve localisation performance when rather large systematic errors are present. GH filter which combined WEO estimations with gyroscope and magnetometer measurements produced better MAE score than WEO on it's own when +/- 6% effective wheelbase error or +/- 3% wheelbase diameter error were present. Additionally, qualitative analysis has shown that there is clear positive relation of WEO performance and the magnitude of systematic errors. There is no such relationship between GH filter solutions and magnitude of errors, proving them more robust. It is expected that use of more precise gyroscope and magnetometer as well as use of more advanced, dynamic, adaptive filters would boost localisation performance gains. It is recommended to explore this in more depth in the future.

REFERENCES

[1] "Robotic Mapping: A Survey", Sebastian Thrun, February 2002

[2] Pololu.com. (2019). Pololu - Romi Encoder Pair Kit, 12 CPR, 3.5-18V. [online] Available at: https://www.pololu.com/product/3542 [Accessed 18 Dec. 2019].

[3] Toledo, J., Pieiro, J., Arnay, R., Acosta, D. and Acosta, L. (2018). Improving Odometric Accuracy for an Autonomous Electric Cart. Sensors, 18(2), p.200.

[4] Borenstein, J.; Feng, L. Measurement and correction of systematic odometry errors in mobile robots. IEEE Trans. Robot. Autom. 1996, 12, 869880.

[5] Martin Brossard, Silvere Bonnabel. Learning Wheel Odometry and IMU Errors for Localization. International Conference on Robotics and Automation (ICRA), May 2019, Montreal, Canada.

[6] Ompusunggu, A. and Bey-Temsamani, A. (2015). 2-Level error (drift) compensation for low-cost MEMS-based inertial measurement unit (IMU). Microsystem Technologies, 22(7), pp.1601-1612.

[7] CEVAs Experts blog. (2019). The Pros, Cons and Uses of Different Gyroscopes - CEVAs Experts blog. [online] Available at: https://www.ceva-dsp.com/ourblog/exploring-the-application-of-gyroscopes/ [Accessed 17 Dec. 2019].

[8] How Good Is Your Gyro [Ask the Experts]. (2010). IEEE Control Systems, 30(1), pp.12-86.

[9] Manon Kok, Jeroen D. Hol and Thomas B. Schon. (2017). Using Inertial Sensors for Position and Orientation Estimation. Foundations and Trends in Signal Processing, Vol. 11: No. 1-2, pp 1-153.

[10] Liu, Z. and Zhu, M. (2014). Calibration and error compensation of magnetometer. The 26th Chinese Control and Decision Conference (2014 CCDC).

[11] Chung, H., Hou, C. C., Chen, Y. (2015). Indoor Intelligent Mobile Robot Localization Using Fuzzy Compensation and Kalman Filter to Fuse the Data of Gyroscope and Magnetometer. IEEE TRANSACTIONS ON INDUSTRIAL ELECTRONICS, VOL. 62, NO. 10

[12] Sawyers, L., Zink, G., Han, D. and Yellapantula, K. (2016). Autonomous Simultaneous Localisation and Mapping Robot.